RSC Advances

A lanthanide coordination polymer is explored as Trp sensor. The possible sensing mechanism is the combination between Trp and Tb^{3+}, which improves the antenna effect.

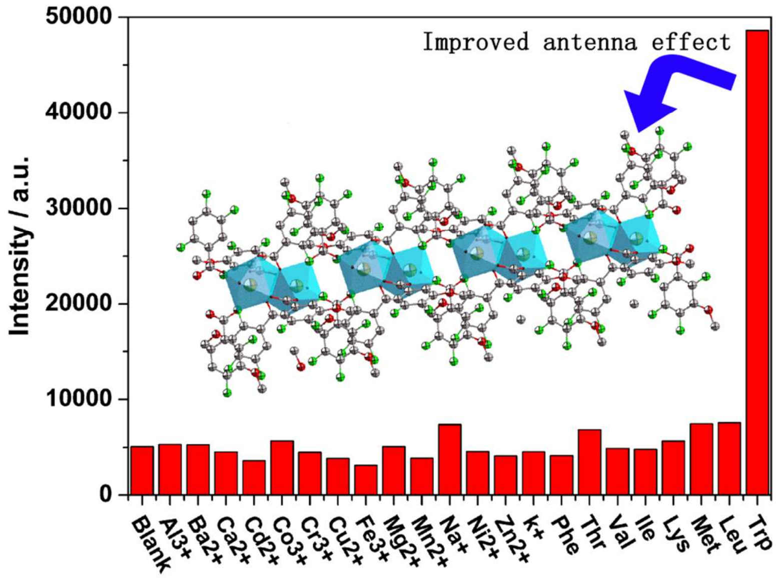

RSC Advances RSC Publishing

ARTICLE

Cite this: DOI: 10.1039/x0xx00000x

Received 00th January 2012,
Accepted 00th January 2012

DOI: 10.1039/x0xx00000x

www.rsc.org/

Highly Luminescent Lanthanide CPs Based on Dinuclear Cluster: Crystal Structure and Sensitive Trp Sensor

Sha-Sha Li,[a] Zhen-Ni Ye,[a] Song-Song Xu,[a] Yu-Jiao Zhang,[a] An-Ran Tao,[a] Min Liu,[a] Cheng-Hui Zeng,[a,b*] Shengliang Zhong,[a*]

Based on a ligand which contains groups of methoxy and fluorine, a series of isostructural lanthanide coordination polymers (CPs) are synthesized, and they are characterized by FT-IR EA, PXRD, TGA and luminescence. Among these complexes, **1** is further characterized by single-crystal diffraction, it crystalizes in the triclinic space group *P-1* (No. 2), with a = 8.8577(8) Å, b = 12.0523(11) Å, c = 13.6494(13) Å, α = 114.2400(10)°, β = 96.3570(10)°, γ = 98.6170(10)°, V = 1289.5(2) $Å^3$ and Z = 2. It is found that **1** and **2** are highly luminescent materials, which show high luminescence QY of 15.45% and 17.51%, respectively. TGA reveals that they are also highly thermostable materials. Sensing experiments reveal that **1** is a highly selective and sensitive tryptophan (Trp) sensor, the responsive behaviour shows excellent linearity in 2.5×10^{-5}-2.5×10^{-4} M, the LOD is as low as 1.0×10^{-6} M. Further study reveals the sensor is applicable in real water sensing. The possible sensing mechanism is the coordination of Trp and Tb^{3+}, which strengthens the antenna effect of **1**.

Introduction

Tryptophan (Trp) is an essential amino acid with diverse physiological roles.[1] It is indispensable in human nutrition for establishing and maintaining a positive nitrogen balance.[2] According to the World Health Organization (WHO), the tryptophan requirement is 4 mg per kg of body per day. Unfortunately, it cannot be synthesized in human body and therefore must be taken from food or pharmaceutical formula. Trp also serves as a precursor for serotonin and melatonin which can improve the sleep, mood, and mental health.[3] When Trp is improperly metabolized, it creates a toxic waste product in the brain, causing hallucinations and delusions. In general, it has been implicated as a probable cause of schizophrenia in people who cannot metabolize it properly. Nowadays, many methods were developed for the determination of tryptophan, including high-performance liquid chromatography (HPLC),[4] HPLC with fluorescence detection, spectrophotometry, liquid chromatography–tandem mass spectrometry, capillary electrophoresis technique, infrared optical sensor, spectrofluorometry, and so on.[5] Although these methods are very useful for the determination of Trp, the majority of them suffer from some disadvantages of long analysis time, tedious extraction process, high costs, and requirement for complicated instruments, and in some cases low sensitivity and selectivity that makes them unsuitable for routine analysis, because these amino acids have the same amino and carboxyl bonded to the same carbon, with very small structure differences, which causes much difficulties in the Trp determination. Therefore, development of a facile, inexpensive, sensitive and accurate analytical method for determination of Trp is of great significance and urgency to people's health.

Lanthanide complexes have been widely used in the area of sensing, electrophysics, magnetism, catalysis, magnetic resonance imaging (MRI), time-resolved microscopy, and so on.[6-9] During the last decade, as an arisen type of sensing materials, lanthanide complexes have been explored to sense many species, such as CO_3^{2-}, OH^-, HSO_4^-, H^+, Ag^+, Cu^{2+}, Mg^{2+}, Zn^{2+}, acetone, halide ions, explosives, proteins, antibiotics, and so on.[10-16] But it was rarely used to detect bio-molecules.

[a] Key Laboratory of Functional Small Organic Molecule, Ministry of Education and Jiangxi's Key Laboratory of Green Chemistry, College of chemistry and chemical engineering, Jiangxi Normal University; Nanchang 330022, P. R. China. E-mail: chenghuizeng@qq.com
[b] Key laboratory of photochemistry, Institute of Chemistry, Chinese academy of sciences.
† Electronic supplementary information (ESI) available: Further details are given in Fig. S1–S4 and Table S1. CCDC:1408145. For ESI and crystallographic data in CIF or other electronic format see DOI: 10.1039/XXXXX

Based on the above considerations, and as further investigation on the lanthanide complex and their application as sensor.[17-22] In this work, ligand of 2,4,5-Trifluoro-3-methoxybenzoic acid (TFMBA), which contains multi-functional groups of fluorine and methoxy, was selected to synthesize lanthanide CPs single crystal. They were characterized by single crystal X-ray diffraction, elemental analysis (EA), powder X-ray diffraction (PXRD), Fourier transform infrared (FT-IR), Thermogravimetric analysis (TGA) and luminescence. **1** was proved to be a highly selective and sensitive Trp sensor. Further investigation indicated the sensor is applicable in real water sensing, and the possible sensing mechanism is suggested.

Experimental

Materials

$Eu(NO_3)_3 \cdot 6H_2O$ was prepared by dissolving Eu_2O_3 (99.9%) with concentrated HNO_3 (68%) and then evaporated at 100 ℃ until the crystal film formed. $Tb(NO_3)_3 \cdot 6H_2O$ and $Gd(NO_3)_3 \cdot 6H_2O$ were obtained from Tb_4O_7 and Gd_2O_3, respectively, with the similar method as $Eu(NO_3)_3 \cdot 6H_2O$. TFMBA (98.0%) was purchased from TCI (Shanghai, China), and used without further purification. NaOH was purchased from Guangzhou Chemical Reagent Factory (Guangzhou, China). Other chemicals (A.R.) are commercially available and used as reveived.

Mother solutions of human necessary amino acids and metal ions were 10^{-3} M water solution. Mother solution of **1** was prepared by dissolving 25 mg **1** in 10 ml DMF (2.5 mg/ml).

Methods and instruments

Single crystal X-ray diffraction data was collected on a Bruker SMART 1000 CCD, with Mo-Kα radiation. The structure was refined by full-matrix least-squares methods with SHELXL-97 module.[23] Phase purity of bulk sample was determined by PXRD, using a DMAX2200VPC diffractometer, at 30 kV and 30 mA. FT-IR was obtained in KBr pellets and recorded on a Nicolet 330 FT-Irspectrometer in 4000-400 cm^{-1}. TGA was recorded on a Netzsch-Bruker TG-209 unit at a heating rate of 10 ℃·min^{-1} in the atmosphere. Luminescence was recorded on an Edinburgh FLS980, with dwell time of 0.20 s, the scan speed was 1 nm/s, at room temperature. Luminescence lifetimes and luminescence QY were also collected by the same Edinburgh FLS980 which equipped with an integrating sphere, and the QY was calculated using the equation method reported by Prof. Melhuish.[24]

Synthesis of 1, 2 and 3

100 mg (0.485 mmol) TFMBA and 10 ml H_2O mixed in a 50 ml beaker, 0.1 M NaOH solution was added to adjust the pH = 6. 0.243 mmol $Ln(NO_3)_3 \cdot 6H_2O$ (**1** = Tb, **2** = Eu and **3** = Gd) was dissolved in 20 ml anhydrous methanol. The upward two solutions were mixed and sealed in a 100 ml beaker by a filter paper. After about one months' evaporation at indoor temperature of about 9-32 ℃, colorless block crystals were got. The crystals were filtered, washed with 6 ml CH_3OH three times and air-dried.

$[TbL_3(H_2O)]_n$ (**1**). Yield: 46.05% based on Tb^{3+}. Anal. Calcd (%):C, 36.38; H, 1.781. Found (%): C, 35.97; H, 1.795. FT-IR (KBr pellet, cm^{-1}, Fig. S1): 3444(s), 3083(w), 2965(w), 1674(m), 1578(s), 1510(m), 1456(m), 1406(s), 1290(w), 1196(m), 1108(s), 922(m), 876(w), 804(m), 771(m), 750(m), 700(w).

$[EuL_3(H_2O)]_n$ (**2**). Yield: 55.29% based on Eu^{3+}. Anal. Calcd (%):C, 36.71; H, 1.797. Found (%): C, 36.14; H, 1.813. FT-IR (KBr pellet, cm^{-1}, Fig. S1): 3456(s), 3084(w), 2965(w), 1670(m), 1576(s), 1516(m), 1457(m), 1403(s), 1288(w), 1196(m), 1108(s), 922(m), 876(w), 804(m), 769(m), 750(m), 700(w).

$[GdL_3(H_2O)]_n$ (**3**). Yield: 53.08% based on Gd^{3+}. Anal. Calcd (%):C, 36.46; H, 1.785. Found (%): C, 36.18; H, 1.797. FT-IR (KBr pellet, cm^{-1}, Fig. S1): 3434(s), 3084(w), 2964(w), 1672(m), 1580(s), 1516(m), 1459(m), 1404(s), 1290(w), 1196(m), 1108(s), 922(m), 876(w), 804(m), 771(m), 750(m), 692(w).

Results and discussion

Crystal Structure

Crystallographic data (table 1) reveals that **1** featuring a 1D CPs of $[TbL_3(H_2O)]_n$ (HL = TFMBA). **1** crystalizes in the Triclinic space group P-1 (No. 2), with a = 8.8577(8) Å, b = 12.0523(11) Å, c = 13.6494(13) Å, α = 114.2400(10)°, β = 96.3570(10)°, γ = 98.6170(10)°, V = 1289.5(2) Å^3 and Z = 2. **1** is constructed by connecting second building units (SBUs, Fig. 1a) of a dinuclear cluster (Fig. 1b), each dinuclear cluster consists two equivalent Tb^{3+}, six deprotonated ligand and two coordinated water, which makes each SBU an electric neutrality unit. The dinuclear cluster connects with each other to form the 1D CPs in the *oa* direction (Fig. 1c). Tb^{3+} coordinates with eight O, one from coordinated water and the rest seven O are from five carboxyls. Eight O around Tb^{3+} arrange in a distorted bi-capped triangular prism, the triangular prism are connected by solid azury line, two caps of O were connected by purple dash line (Fig. S2). Eight bond lengths of Tb-O are in 2.276(2)-2.592(2) Å, which are in the normal bond length range of Ln-O.[25-27] Moreover, the Tb···Tb distance bridged by two carboxyl O and two carboxyl is as short as 3.9452(4) Å, which is much shorter than the Tb···Tb distance of 4.921 Å which bridged by carboxyl.[21] The short Tb···Tb distance may due to the two strong bond strength of carboxyl O, which pulls the two Tb^{3+} together and make the whole structure more rigid.

In **1**, ligands have two coordination modes (Fig. S3). The first type is a carboxyl chelates to Tb^{3+} and bridge two Tb^{3+} (μ_2-η^2-η^1), the other is a carboxyl bridge two adjacent Tb^{3+} that adopting the coordinating mode of μ_2-η^1-η^1. The 1D structure is connected to form 3D structure, by weak hydrogen bond and Van der Waals force (VDW). More information about selected bond lengths and angles for **1** is listed in Table S1 (ESI†).

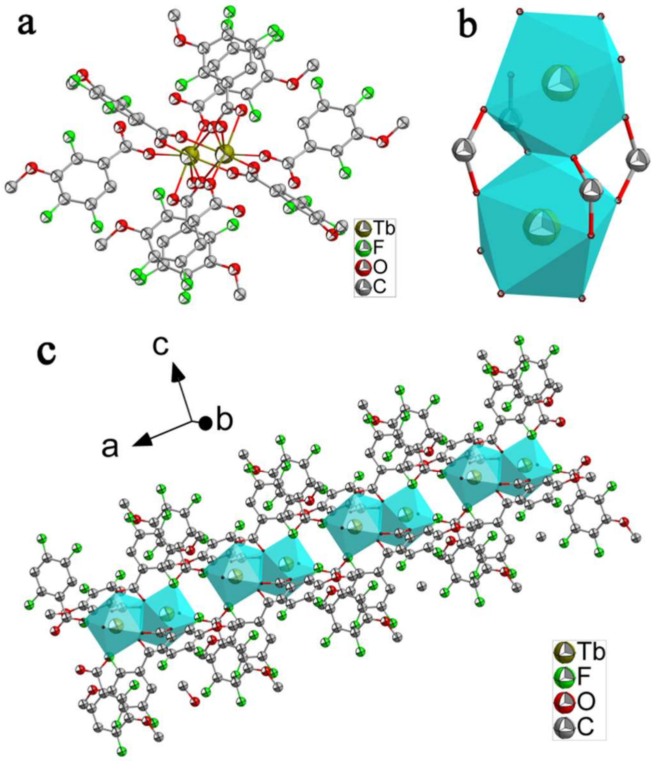

Figure 1. a) SBU in **1**; b) di-nuclear cluster of the SBU; c) 1D CPs structure of **1** in *oa* direction.

Table 1. Crystallographic data of **1** (CCDC: 1408145).

Complex	**1**
Empirical formula	$C_{24}H_{14}F_9O_{10}Tb$
Formula weight	792.28
Temperature / K	296(2) K
Wavelength / Å	0.71073
Crystal system	Triclinic
Space group	P-1
a / Å	8.8577(8)
b / Å	12.0523(11)
c / Å	13.6494(13)
α / °	114.2400(10)
β / °	96.3570(10)
γ / °	98.6170(10)
V / $Å^3$	1289.5(2)
Z	2
Calculated density / $mg·m^{-3}$	2.041
F(000)	768
Crystal size/mm	0.17×0.16×0.12
Data/restraints / parameters	4525/406/407
Goodness-of-fit on F^2	1.065
Final R indices	R1 = 0.0218
[I > 2sigma(I)]	wR2 = 0.0569

PXRD

Experimental PXRD patterns' peak positions of bulk sample **1-3** (**1** = Tb, **2** = Eu and **3** = Gd) correspond well with each other, and also match well with the results simulated from the single-crystal data **1**, indicating the high phase purity of powder samples **1-3**, and also confirm **1-3** are isostructural (Fig. 2).

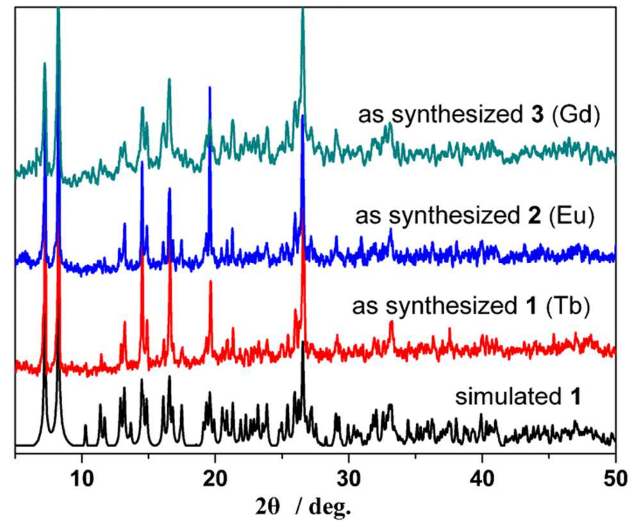

Figure 2. PXRD patterns of simulated **1** and as synthesized **1-3**.

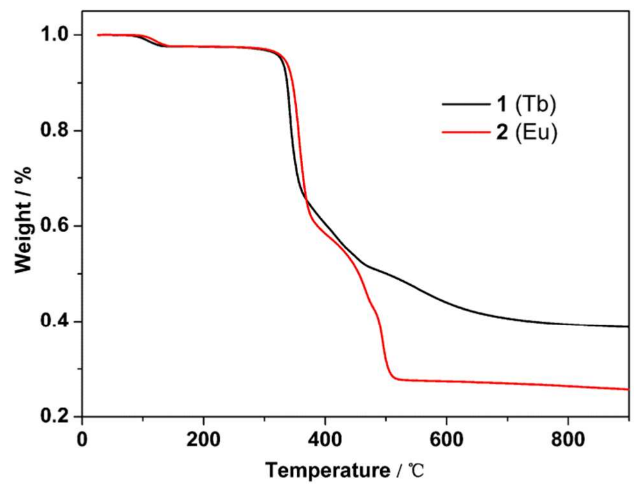

Figure 3. TGA of **1** and **2** in the atmosphere.

TGA

Since **1-3** are isostructures, complex **1** and **2** were selected as representative for thermogravimetric analysis (TGA) to examine the thermal stabilities of the three complexes (Fig. 3). 2.71% and 2.87% weight loss before 132 and 140 °C for **1** and **2**, respectively, which is attributed to the release of coordination H_2O (calculated 2.27% and 2.29% for **1** and **2**, respectively). The TGA curve reveals that **1** and **2** begin to decompose and both show two evident weight loss from 322 °C, which corresponding to the collapsion of the structure. TGA result implies that **1** and **2** are thermo-stable under 322 °C in the air, which is more thermo-stable than another highly thermo-stable (stable up to 290 °C) Metal–Organic Frameworks.[16]

Luminescence

Luminescence of solid sample **1** and **2** were tested at the room temperature. When fixing the strongest emission at 546 nm ($^5D_4 \rightarrow {}^7F_5$), the excitation spectrum of **1** displays a broad band covering from 235 to 370 nm (Fig. 4), which suggests **1** is a broad wavelength excitation material. The emission spectrum was recorded at the best excitation of 303 nm. Narrow line emissions at 488, 546, 584, and 622 nm are the characteristic emissions of Tb^{3+}, corresponding to the transitions of $^5D_4 \rightarrow {}^7F_6$, $^5D_4 \rightarrow {}^7F_5$, $^5D_4 \rightarrow {}^7F_4$, and $^5D_4 \rightarrow {}^7F_3$, respectively (Fig. 4).[28-31]

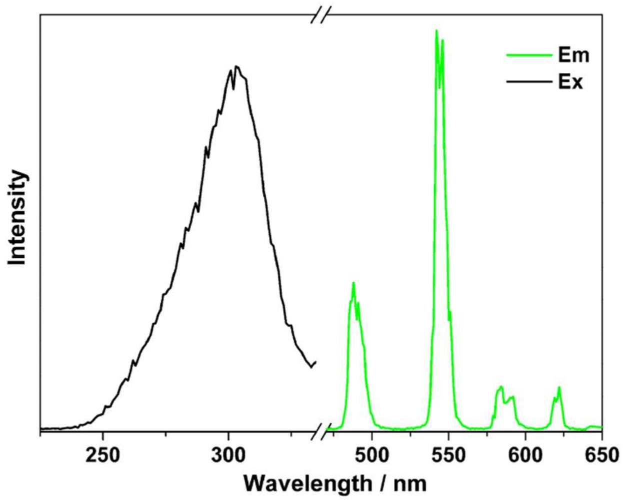

Figure 4. Excitation and emission spectra of **1** in the solid state at room temperature.

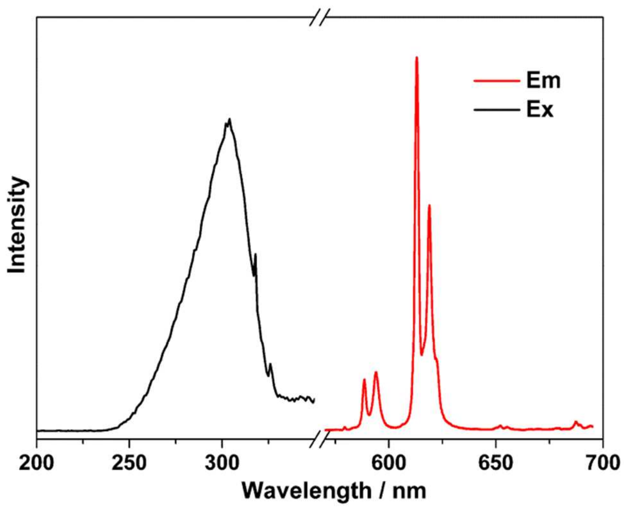

Figure 5. Excitation and emission specta of **2** in the solid state at room temperature.

For **2**, when fixing the strongest emission at 619 nm ($^5D_0 \rightarrow {}^7F_2$), the excitation spectrum of **1** displays a broad band covering from 235 to 335 nm (Fig. 5). The emission spectrum was recorded at the best excitation of 304 nm, which has very small difference with **1** (Ex = 303 nm), and this small difference may due to the error which induced by the instrument. Narrow line emissions at 589, 619, 650 and 689 nm are the characteristic emissions of Eu^{3+}, corresponding to the transitions of $^5D_0 \rightarrow {}^7F_1$, $^5D_0 \rightarrow {}^7F_2$, $^5D_0 \rightarrow {}^7F_3$ and $^5D_0 \rightarrow {}^7F_4$, respectively (Fig. 5).[16]

The total luminescence QY of **1** (Tb^{3+}-centered complex) and **2** (Eu^{3+}-centered complex), are 15.45% and 17.51%, respectively, under the best excitations of 303 and 304 nm, and the QY of **2** is larger than **1**. The luminescence QY of Eu^{3+}-centered complex **2** is a little lower than anther reported Eu^{3+} based highly luminescent materials.[32] The high luminescence QY may due to that there are only one C-H on the benzene, other positions on carboxyl are fluorine or methoxy, this decrease the oscillation in the complex.[27] **1** and **2** are isostructural, and the overall luminescence QY of **2** is larger than **1**, which indicates the energy transfer from the ligand to Eu^{3+} is more efficient than to Tb^{3+}.

Luminescence lifetimes of **1** and **2** were investigated in solid state. The luminescence decays were monitored at 546 and 619 nm, for **1** and **2**, respectively Fig. 6. **1** and **2** followed single exponential decay law, and the equation of $I_t = A_0 + A_1 \times \exp(-t/\tau)$ (τ is the luminescence lifetime, A_0 and A_1 are the weighting parameters) was utilized for fitting the luminescence decay curves, lifetime values were determined to be 0.860 and 0.507 ms for **1** and **2**, respectively.

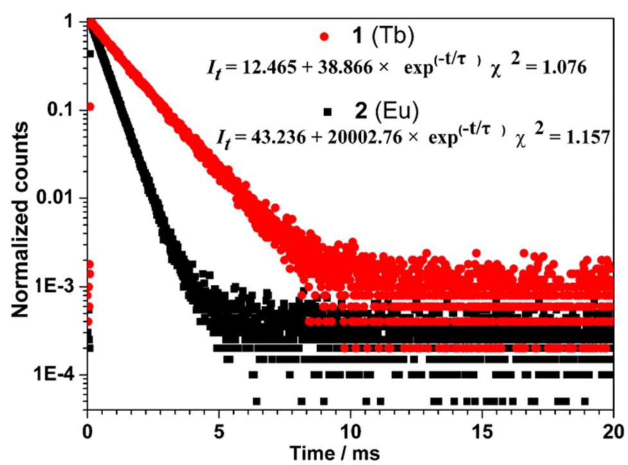

Figure 6. Luminescence decay of **1** and **2** in the solid state at room temperature.

To investigate the energy transfer efficiency in complex **1** and **2**, energy levels of the relevant electronic states should be estimated. On account of difficulty in observing phosphorescence spectrum of the ligand in **1** and **2**, emission spectrum of Gd^{3+} complex (**3**) at 77 *K* can be used to estimate the triplet state energy level. Because the lowest excited energy level of $^6P_{7/2}$ of Gd^{3+} is too high to accept energy transfer from the ligand, and the triplet state energy level of ligand will not significantly affected by the Gd^{3+}. Fig. S4 shows the phosphorescence of **3** at 77 K with excitation wavelength at 353 nm, with the best phosphorescence emission at 395 nm, which corresponds to the triplet energy level of ligand at 25 316 cm^{-1}. The energy gap between triplet energy level of ligand and $^5D_4$ level of Tb^{3+} (20540 cm^{-1}) is 4776 cm^{-1}, which is good news for energy transfer through the $^5D_4$–$^7F_6$ transition, because an energy gap of 3500 cm^{-1} or higher is necessary to facilitate efficient and irreversible energy transfer for terbium complexes,[18] this is consistent with the highly luminescent QY result of **1**.

Sensor

Luminescent lanthanide complexes have been used to detect many species, such as CO_3^{2-}, HSO_4^-, OH^-, H^+, Ag^+, Hg^{2+}, Pb^{2+}, Zn^{2+}, Cu^{2+}, Mg^{2+}, Mn^{2+}, O_2, halide ions, acetone, highly explosives, proteins, amino acids, and so on.[32-36] There are methoxyl and fluorine in TFMBA, and they may combine with other species by weak hydrogen bond and/or halogen hydrogen bond, which would result in variable luminescence, thus, the sensing property of **1** was investigated in detail.

One crucial factor effecting the sensing is the pH of the sensing system. Hence, luminescence (at 546 nm) of the mother solution **1** at different pH (1-13) was tested, with the pH adjusted by HNO_3 or NaOH. It was found that the luminescence was the strongest at pH = 4 (Fig. 7). Therefore, the sensing was implemented at pH = 4, in the water solution.

An effect of reaction time is the concentration of **1**, thus, reaction of different concentration **1** (0.5-4 mg/ml) and 31.2 μM Trp were performed (Fig. S5). Results found that the luminescence intensity increased with the concentration of **1** increasing, therefore, 2.5 mg/ml of solution was adopted in the sensing studies, because the detecting result is not obvious when the concentration of **1** is lower, however, longer reaction time needed while at too large concentration of **1** is too high. Another effect for reaction is the temperature, the real application is usually at room temperature, hence, the temperature effect was not investigated.

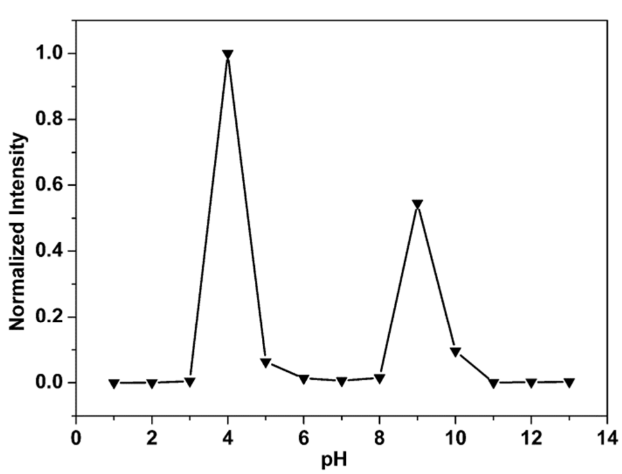

Figure 7. Luminescence of the sensing solution at 546 nm, at different pH.

The detecting were processed at the room temperature, 0.1 ml 1 mM metal ion solutions were added into 0.1 ml 2.5 mg/ml **1** DMF solution, and 3 ml water was added to form a 31.2 μM metal ion solution. The mixtures were placed at the room temperature to react for 2 h, and the sensing result can be seen in Fig. 8. It displays the emission change of Tb^{3+} when reacting with various metal (M) ions ($M(NO_3)_X$ or MCl_X) (M = Al^{3+}, Ba^{2+}, Ca^{2+}, Cd^{2+}, Co^{3+}, Cr^{3+}, Cu^{2+}, Fe^{3+}, Mg^{2+}, Mn^{2+}, Na^+, Ni^{2+}, Zn^{2+} and K^+) and 8 human essential amino acids (Trp, Phe, Thr, Val, Ile, Lys, Met and Leu). Among the 14 metal ions and 8 human necessary amino acids, only Trp enhanced the Tb^{3+} centered luminescence (about 9 times as that of blank), other 14 ions and 7 amino acids showed nearly no effect on the luminescence intensity. The histogram shows more obviously about the luminescence changes, when **1** reacting with different ions (Fig. S6).

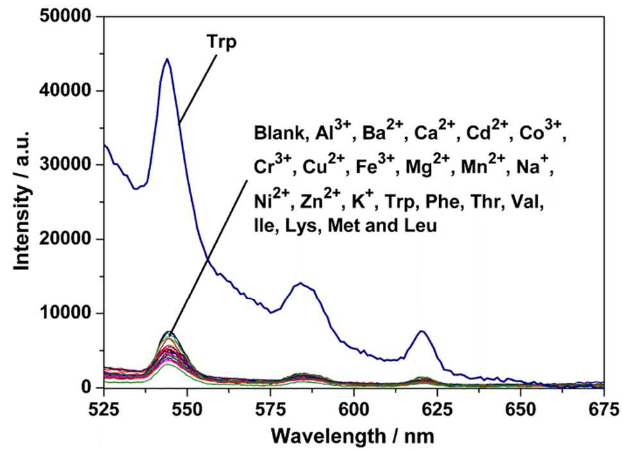

Figure. 8 The luminescence of **1** reacted with different metal ions of Al^{3+}, Ba^{2+}, Ca^{2+}, Cd^{2+}, Co^{3+}, Cr^{3+}, Cu^{2+}, Fe^{3+}, Mg^{2+}, Mn^{2+}, Na^+, Ni^{2+}, Zn^{2+} and K^+, and 8 human essential amino acids of Trp, Phe, Thr, Val, Ile, Lys, Met and Leu.

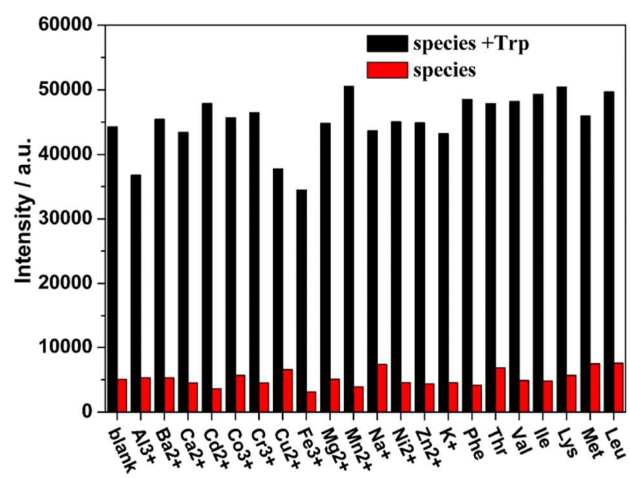

Figure 9. Luminescence of **1**+Trp at the presence of 10 equiv. other species.

One disadvantage of the current luminescent sensors is that they are easily disturbed by other species. To investigate whether sensor **1** is specific for Trp, we measured the luminescence response of this sensing system with 14 common ions (Al^{3+}, Ba^{2+}, Ca^{2+}, Cd^{2+}, Co^{3+}, Cr^{3+}, Cu^{2+}, Fe^{3+}, Mg^{2+}, Mn^{2+}, Na^{+}, Ni^{2+}, Zn^{2+} and K^{+}), and 7 common human necessary amino acids (Phe, Thr, Val, Ile, Lys, Met and Leu) mixed with Trp, under the same conditions. As shown in Fig. 9, Trp could induce a drastic luminescence increase in the presence of 10 equiv. 14 metal ions or 7 amino acids. The result of compete experiment indicates that **1** is highly selective towards Trp over other species.

LOD and Linearity

It was found that the luminescence increased obviously when 1.0×10^{-6} M Trp reacted with **1** for 2 h, the ratio of increased luminescence to noise is larger than 3 ($\Delta S/N > 3$) (Fig. 10). Thus, the LOD is an ultrahigh sensitive value of 1.0×10^{-6} M. The LOD value is more sensitive than a recently reported electrochemical method (33×10^{-6} M),[38] but less sensitive than the value reported by Prof. Li (LOD = 2×10^{-9} M) and Prof. Shuang (LOD = 5×10^{-7} M).[5, 39]

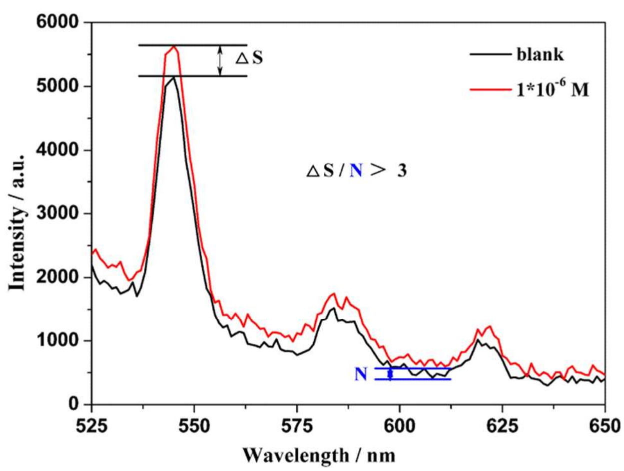

Figure. 10 The LOD of **1** to Trp is 1.0×10^{-6} M.

Fig. 11 shows the luminescence intensity at 546 nm increased obviously, when the Trp concentration was in 1.0×10^{-6} - 7.5×10^{-4} M. Further investigation found the luminescence intensity has excellent linear relationship with the Trp concentration in 2.5×10^{-5} - 2.5×10^{-4} M, they fit a linear formula of Y = -1880.6X + 14117 (X represents the Trp concentration and Y represents luminescence intensity), the R^2 is as large as 0.9909.

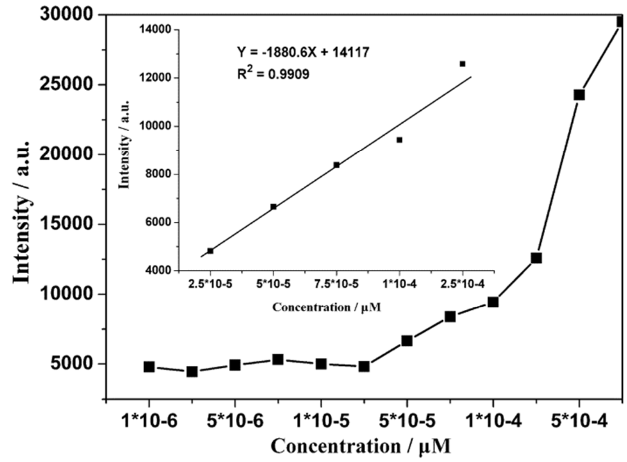

Figure 11. Luminescence (546 nm) change while the concentration of Trp is in 1.0×10^{-6}-7.5×10^{-4} M, and the insert shows the excellent linearity in 2.5×10^{-5}-2.5×10^{-4} M.

Possible Sensing Mechanism

Among the 14 metal ions of Al^{3+}, Ba^{2+}, Ca^{2+}, Cd^{2+}, Co^{3+}, Cr^{3+}, Cu^{2+}, Fe^{3+}, Mg^{2+}, Mn^{2+}, Na^{+}, Ni^{2+}, Zn^{2+} and K^{+}, and 8 human necessary amino acids of Trp, Phe, Thr, Val, Ile, Lys, Met and Leu, only Trp and Phe has chromophore group (potential antenna for Tb^{3+}), Trp contain the group of indole, the N on the indole group may coordinate to Tb^{3+}, to act as another antenna, besides the main ligand of TFMBA. However, the benzene on the Phe can't act as efficient antenna for Tb^{3+} for two reasons, firstly, the benzene can't coordinate to Tb^{3+} directly; secondly, even the carboxyl in Phe can coordinate to Tb^{3+}, the energy transfer way is too far to form efficient energy transfer to Tb^{3+}. Therefore, the sensing mechanism may due to the coordination of Trp and Tb^{3+} in **1**, which strengthens the antenna effect of **1**.

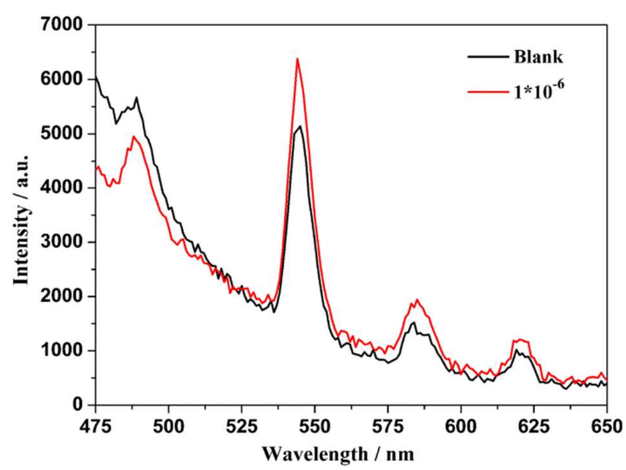

Figure 12. Real water (Yao lake water) sensing when the Trp is 1.0×10^{-6} M.

Sensing in real water and in PBS buffer solution

To evaluate whether the luminescent sensor **1** is applicable to real water samples, Yao lake (in Nanchang City) water was analyzed by **1**. The sensing results show that the Yao Lake water gives no obvious fluorescence increase while comparing to deionized water, and the sensing is not recovered. Nevertheless, the luminescence increased, while 0.1 ml 2.5 mg/ml **1** was added into 3.1 ml 1.0×10^{-6} M Trp solutions which prepared by Yao Lake water. The increased luminescence (ΔS) is three times as the noise (N) (Fig. 12). The result revealed the sensor could be used in real water sensing for Trp. The sensing results indicate the Trp concentration is lower than 1.0×10^{-6} M in Yao lake water.

Trp is a bio-molecule and exits in the blood, interstitial fluid, in the cell, and so on. The pH of these environments are about 7, therefore, the sensing was further measured in PBS buffer solution (pH = 7.4) usually applied in cell culture and molecular cloning.[37] 0.1 ml 1 mM metal ion or amino acid solutions were added into 0.1 ml 2.5 mg/ml **1** DMF solution, and 3 ml PBS buffer solution was added to form a 31.2 μM metal ion or amino acid solutions, the mixtures were placed at the room temperature to react for 2 h. The sensing result can be seen in Fig. S7. Among the 14 metal ions (Al^{3+}, Ba^{2+}, Ca^{2+}, Cd^{2+}, Co^{3+}, Cr^{3+}, Cu^{2+}, Fe^{3+}, Mg^{2+}, Mn^{2+}, Na^{+}, Ni^{2+}, Zn^{2+} and K^{+}) and 8 human necessary amino acids (Trp, Phe, Thr, Val, Ile, Lys, Met and Leu), only Trp effet the Tb^{3+} centered luminescence greatly (about 9 times as that of blank), other 14 ions and 7 amino acids showed nearly no effect on the luminescence intensity. The result indicates that **1** is a highly selective Trp sensor in biological PBS solution.

Conclusion

In conclusion, a series of isostructural lanthanide CPs are synthesized based on TFMBA, they are characterized by FT-IR EA, PXRD, TGA and luminescence. Among these complexes, exact structure of **1** is got by single-crystal diffraction. It is found that **1** and **2** are broad wavelength absorption, highly thermostable and highly luminescent materials. Further study reveal that **1** is a highly selective and sensitive Trp sensor, the responsive behavior shows excellent linearity in 2.5×10^{-5} - 2.5×10^{-4} M, the LOD is 1.0×10^{-6} M. More interestingly, the sensor is applicable in real water sensing. The possible sensing mechanism is the coordination of Trp and Tb^{3+}, which results in the strengthened antenna effect of **1**. Further work to lower down the LOD for real water sensing, and the sensing of Trp in the body fluid is under way.

Acknowledgements

The authors acknowledge the financial support of the Open Project Program of Key Laboratory of Functional Small Organic Molecule, Ministry of Education (No. KLFS-KF-201422), and the 973 program in China (2013CB933503), the National Natural Science Foundation of China (Nos. 21201089, 21261010, 61201104), Jiangxi Provincial Education Department (No. KJLD13021) and Jiangxi Provincial Department of Science and Technology (No. 20144BCB23039).

Reference

1. M. Mazloum-Ardakani, H. Beitollahi, M. K. Amini, F. Mirkhalaf and B.-F. Mirjalili, *Biosens. Bioelectron.*, 2011, 26, 2102-2106.
2. B. Fang, Y. Wei, M. Li, G. Wang and W. Zhang, *Talanta*, 2007, 72, 1302-1306.
3. A. R. Fiorucci and E. T. G. Cavalheiro, *J. Pharm. Biomed. Anal.*, 2002, 28, 909-915.
4. W. Lian, D. J. Ma, X. Xu, Y. Chen and Y. L. Wu, *J. Digest. Dis.*, 2012, 13, 100-106.
5. J. Li, D. Kuang, Y. Feng, F. Zhang, Z. Xu, M. Liu and D. Wang, *Biosens. Bioelectron.*, 2013, 42, 198-206.
6. L. Armelao, S. Quici, F. Barigelletti, G. Accorsi, G. Bottaro, M. Cavazzini and E. Tondello, *Coord. Chem. Rev.*, 2010, 254, 487-505.
7. L. Winkless, R. H. C. Tan, Y. Zheng, M. Motevalli, P. B. Wyatt and W. P. Gillin, *Appl. Phys. Lett.*, 2006, 89, 111115.
8. Y. Hasegawa and T. Nakanishi, *RSC Adv.*, 2015, 5, 338-353.
9. Z. Ahmed and K. Iftikhar, *RSC Adv.*, 2014, 4, 63696-63711.
10. B. Chen, S. Xiang and G. Qian, *Acc. Chem. Res.*, 2010, 43, 1115-1124.
11. L. Zhao, Y. Liu, C. He, J. Wang and C. Duan, *Dalton Trans.*, 2014, 43, 335-343.
12. M. L. Aulsebrook, B. Graham, M. R. Grace and K. L. Tuck, *Tetrahedron*, 2014, 70, 4367-4372.
13. Q.-B. Bo, H.-T. Zhang, H.-Y. Wang, J.-L. Miao and Z.-W. Zhang, *Chem. Eur. J.*, 2014, 20, 3712-3723.
14. H.-M. Wang, Y.-Y. Yang, C.-H. Zeng, T.-S. Chu, Y.-M. Zhu and S. W. Ng, *Photoch. Photobio. Sci.*, 2013, 12, 1700-1706.
15. Y. Liu, M. Chen, T. Cao, Y. Sun, C. Li, Q. Liu, T. Yang, L. Yao, W. Feng and F. Li, *J. Am. Chem. Soc.*, 2013, 135, 9869-9876.
16. S.-N. Zhao, X.-Z. Song, M. Zhu, X. Meng, L.-L. Wu, S.-Y. Song, C. Wang and H.-J. Zhang, *RSC Adv.*, 2015, 5, 93-98.
17. K. Zheng, K.-L. Lou, C.-H. Zeng, S.-S. Li, Z.-W. Nie and S. Zhong, *Photochem. Photobiol.*, 2015, 10.1111/php.12460.
18. Z.-Q. Yan, X.-T. Meng, R.-R. Su, C.-H. Zeng, Y.-Y. Yang, S. Zhong and S. W. Ng, *Inorg. Chim. Acta*, 2015, 432, 41-45.
19. M. Shi, C. Zeng, L. Wang, Z. Nie, Y. Zhao and S. Zhong, *New J. Chem.*, 2015, 39, 2973-2979.
20. Y. Sun, W. Feng, P. Y. Yang, C. H. Huang and F. Y. Li, *Chem. Soc. Rev.*, 2015, 44, 1509-1525.
21. Z.-W. Nie, S.-S. Li, C.-H. Zeng, L. Wang, Y. Li, S.-G. Yin and S.-L. Zhong, *Z. Anorg. Allg. Chem.*, 2014, 640, 2255 - 2260.
22. C.-H. Zeng, F.-L. Zhao, Y.-Y. Yang, M.-Y. Xie, X.-M. Ding, D.-J. Hou and S. W. Ng, *Dalton Trans.*, 2013, 42, 2052-2061.
23. G. M. Sheldrick, SADABS, University of G¨ ottingen, G¨ ottingen, Germany1997.
24. W. H. Melhuish, *J. Phys. Chem.*, 1961, 65, 229-&.

25. W.-B. Chen, Z.-X. Li, Z.-J. Ouyang, W.-N. Lin, L. Yang and W. Dong, *RSC Adv.*, 2014, 4, 61104-61113.
26. B. Ji, D. Deng, J. Ma, C. Sun and B. Zhao, *RSC Adv.*, 2015, 5, 2239-2248.
27. C.-H. Zeng, J.-L. Wang, Y.-Y. Yang, T.-S. Chu, S.-L. Zhong, S. W. Ng and W.-T. Wong, *J. Mater. Chem. C*, 2014, 2, 2235-2242.
28. Y. Yue, Y. Liang, H. Wang, L. Feng, S. Feng and H. Lu, *Photochem. Photobiol.*, 2013, 89, 5-13.
29. Y. Mei and B. Yan, *Photochem. Photobiol.*, 2014, 90, 1462-1466.
30. Q.-P. Li and B. Yan, *Photochem. Photobiol.*, 2014, 90, 22-28.
31. J. Cuan and B. Yan, *RSC Adv.*, 2014, 4, 1735-1743.
32. Y.-M. Zhu, C.-H. Zeng, T.-S. Chu, H.-M. Wang, Y.-Y. Yang, Y.-X. Tong, C.-Y. Su and W.-T. Wong, *J. Mater. Chem. A*, 2013, 1, 11312-11319.
33. Z. Hao, X. Song, M. Zhu, X. Meng, S. Zhao, S. Su, W. Yang, S. Song and H. Zhang, *J. Mater. Chem. A*, 2013, 1, 11043-11050.
34. Y. Cui, B. Chen and G. Qian, *Coord. Chem. Rev.*, 2014, 273, 76-86.
35. B. Wang, Q. Huang and C. Zeng, *Research on the Mechanisms of Integration of Industry Chains Driven by Informatization*, 2010.
36. G. L. Law, T. A. Pham, J. D. Xu and K. N. Raymond, *Angew. Chem. Int. Ed.*, 2012, 51, 2371-2374.
37. S. Q. Wang, Q. H. Wu, H. Y. Wang, X. X. Zheng, S. L. Shen, Y. R. Zhang, J. Y. Miao and B. X. Zhao, *Biosens. Bioelectron.*, 2014, 55, 386-390.
38. D. Guo, Y. Huang, C. Chen, Y. Chen and Y. Fu, *New J. Chem.*, 2014, 38, 5880-5885.
39. H. Wang, Y. Zhou, Y. Guo, W. Liu, C. Dong, Y. Wu, S. Li and S. Shuang, *Sens. Actuators, B*, 2012, 163, 171-178.